AFRL-DE-PS-
TP-2006-1007

DESIGN, FABRICATION, AND VALIDATION OF AN ULTRA-LIGHTWEIGHT MEMBRANE MIRROR (Conference Proceedings)

James D. Moore, Brian G. Patrick, Surya Chodimella (SRS Technologies)
Dan K. Marker, Brett deBlonk (AFRL)

1 August 2005

Technical Paper

APPROVED FOR PUBLIC RELEASE; DISTRIBUTION IS UNLIMITED.

AIR FORCE RESEARCH LABORATORY
Directed Energy Directorate
3550 Aberdeen Ave SE
AIR FORCE MATERIEL COMMAND
KIRTLAND AIR FORCE BASE, NM 87117-5776

REPORT DOCUMENTATION PAGE

Form Approved
OMB No. 0704-0188

1. REPORT DATE (DD-MM-YYYY)	2. REPORT TYPE	3. DATES COVERED (From - To)
01-08-2005	Technical Paper Postprint	1 March 2003 - 5 July 05

4. TITLE AND SUBTITLE
Design, Fabrication, and Validation of an Ultra-Lightweight Membrane Mirror (Conference Proceedings)

5a. CONTRACT NUMBER
F29601-03-C-0040 (DF297273)

5b. GRANT NUMBER

5c. PROGRAM ELEMENT NUMBER
65502F

6. AUTHOR(S)
James D. Moore, Brian G. Patrick, Surya Chodimella
Dan K. Marker*, Brett deBlonk*

5d. PROJECT NUMBER
3005

5e. TASK NUMBER
DP

5f. WORK UNIT NUMBER
BE

7. PERFORMING ORGANIZATION NAME(S) AND ADDRESS(ES)
SRS Technologies
500 Discovery Drive
Huntsville, AL 35806

8. PERFORMING ORGANIZATION REPORT NUMBER

9. SPONSORING / MONITORING AGENCY NAME(S) AND ADDRESS(ES)
*Air Force Research Laboratory
3550 Aberdeen Avenue SE
Kirtland AFB, NM 87117-5776

10. SPONSOR/MONITOR'S ACRONYM(S)

11. SPONSOR/MONITOR'S REPORT NUMBER(S)
AFRL-DE-PS-TP-2006-1007

12. DISTRIBUTION / AVAILABILITY STATEMENT
Approved for Public Release; Distribution is Unlimited.

13. SUPPLEMENTARY NOTES Author final manuscript, Pub. in Proceedings of SPIE 50th Annual Meeting, Photonics, Vol. 5894, August 2005.

14. ABSTRACT

Large aperture optical quality primary mirrors have been developed which are extremely lightweight (areal densities less than 1kg/m2) made from stretched reflective polymer membranes. However, aberrations induced by boundary support errors and pressurization of a flat membrane do not produce a perfect parabolic shape. Modeling studies have shown that active boundary control can be very effective in correcting certain types of figure errors typically seen in membrane mirrors. This paper validates these design studies by applying boundary control on a 0.25-meter pressure augmented membrane mirror (PAMM). The 0.25-meter PAMM was fabricated as a pathfinder for a larger prototype. A combination of displacement actuators and electrostatic force actuators were used to control the shape of the mirror. A varied thickness stress coatings prescription was developed by a SRS/AFRL team using nonlinear membrane theory. Based on modeled data, the stress coating should force the membrane into a parabolic shape when pressurized, as opposed to a spherically aberrated shape characteristic of a pressurized flat membrane. Test data from the 0.25-meter PAMM proved that the varied thickness stress coating allows for a better shape than the uniform coating.

15. SUBJECT TERMS
Membrane mirror, boundary control, modeling, validation, stress coating

16. SECURITY CLASSIFICATION OF:			17. LIMITATION OF ABSTRACT	18. NUMBER OF PAGES	19a. NAME OF RESPONSIBLE PERSON
a. REPORT	b. ABSTRACT	c. THIS PAGE			Dan K. Marker
Unclassified	Unclassified	Unclassified	SAR	11	19b. TELEPHONE NUMBER (include area code) 505-846-2871

Design, Fabrication, and Validation of an Ultra-Lightweight Membrane Mirror

Surya Chodimella, James D. Moore, Brian G. Patrick
SRS Technologies, Huntsville AL, USA 35806

Brett deBlonk, Dan K. Marker
Air Force Research Lab, Kirtland AFB

ABSTRACT

Large aperture optical quality primary mirrors have been developed which are extremely lightweight (areal densities less than 1kg/m^2) made from stretched reflective polymer membranes. However, aberrations induced by boundary support errors and pressurization of a flat membrane do not produce a perfect parabolic shape. Modeling studies have shown that active boundary control can be very effective in correcting certain types of figure errors typically seen in membrane mirrors. This paper validates these design studies by applying boundary control on a 0.25-meter pressure augmented membrane mirror (PAMM). The 0.25 meter PAMM was fabricated as a pathfinder for a larger prototype. A combination of displacement actuators and electrostatic force actuators were used to control the shape of the mirror. A varied thickness stress coating prescription was developed by a SRS/AFRL team using nonlinear membrane theory. Based on modeled data, the stress coating should force the membrane into a parabolic shape when pressurized, as opposed to a spherically aberrated shape characteristic of a pressurized flat membrane. Test data from the 0.25-meter PAMM proved that the varied thickness stress coating allows for a better shape than the uniform coating.

Keywords: Membrane mirror, boundary control, modeling, validation, stress coating

1. INTRODUCTION

The use of integrated modeling techniques including structural and optical analyses enables design of high performance optical systems. Design studies conducted using ALGOR finite element software and the Integrated Optical Design Analysis Program (IODA) developed by SRS predicted that boundary actuation could provide very good control authority over symmetric Zernike terms[1]. In these studies, various boundary control configurations were compared with each other relative to their ability to correct typical aberrations and improve surface figure. The designs that had the best performance were the options of using linear displacement actuators for out-of-plane boundary warping of the membrane support ring and radial control of the membrane. Testing to validate this design was performed on a 0.25m mount (**Figure 1**) that utilized linear displacement actuators, for both out-of-plane and radial control of the boundary support. Test data of this 0.25m mount will be used to refine the finite element models to support the design of a 0.75-meter PAMM. The 0.75-meter PAMM will incorporate linear displacement actuators for out-of-plane boundary warping of the membrane support ring, and radial membrane control will be accomplished by electrostatic pressure actuators located circumferentially around the outer diameter of the membrane just inside of the boundary support ring. The software and control equipment that will be used to electrostatically control the boundary of the 0.75m system was assembled and tested by applying it to a full aperture control on the 0.25m PAMM.

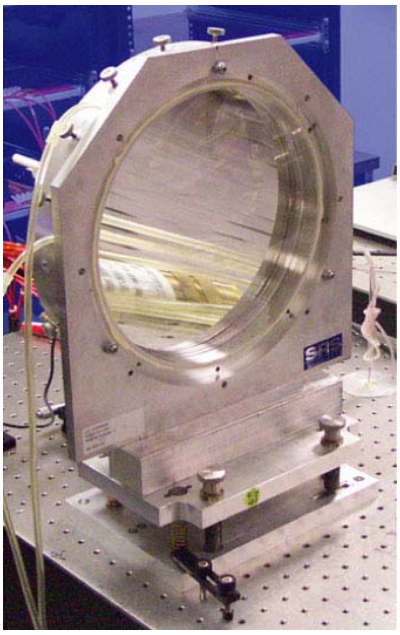

Figure 1. 0.25-meter Pressure Augmented Membrane Mirror

Active boundary control is very promising and studies predict good control over astigmatism and coma aberrations. However, the primary disadvantages of boundary control are the lack of adequate control authority over spherical aberration and changes in focal length. In most cases, a shift in focal length can be corrected by changing the distance between primary and secondary mirror. Global shape control can be utilized to correct for spherical aberration, but challenges such as increase in the weight of reaction structure and number of actuators with increasing apertures limit this approach to smaller diameter mirrors using standard actuator techniques. However, the spherical aberration can be reduced in order to be realized in the downstream optics. A varied thickness stress coating prescription was developed by SRS/AFRL using the nonlinear membrane theory, and initial test results on the 0.25-meter PAMM indicates reduced spherical aberration when pressurized.

2. MODELING VALIDATION

A 0.25m mirror mount was designed that utilized radial boundary control coupled with boundary warping to demonstrate the feasibility of boundary control and validate the design analysis. The mount has a split lenticular setup, allowing one canopy and many membrane mirrors that can be interchanged. The mount has a clear aperture of 0.25m with the entire mount having an outer diameter of 0.33m. This mount employed a series of boundary actuators that allow radial and out-of-plane control as shown in **Figure 2**. The mount used a CP1-DE membrane coated with a uniform layer of aluminum and tests were performed using white-light Ronchi test measurements to measure the figure accuracy of the pressurized membrane. The control authority is measured by the residual rms error after implementing the boundary control. **Figure 3** shows the Ronchi test schematic as well as the actual test setup in the SRS optics lab.

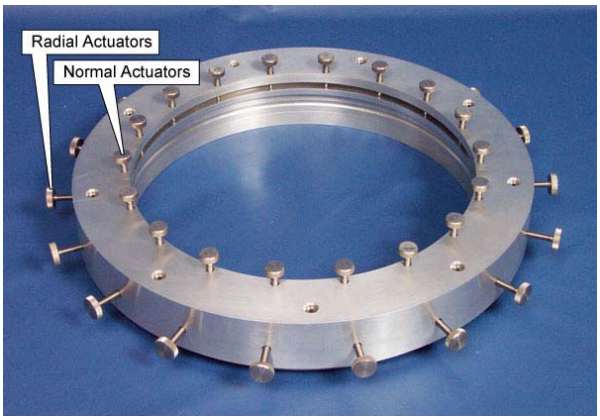

Figure 2. 0.25meter Mount with Boundary Actuators

The mirror was pressurized to the design pressure and measured Ronchi data was analyzed with the in-house SRS-THIN software. SRS-THIN uses a shear analysis technique to calculate optical path difference (OPD) surface plots and Zernike coefficients for the Ronchigram data. The data shown in **Figure 4** defines the characteristic shape error of the PAMM after subtracting the focus and rigid body terms from the Zernike surface. This is the figure error measured from a flat reference. The mirror has a high amount of spherical aberration, which is as expected. Results from finite element modeling showed that astigmatism can be corrected with the normal actuators and coma aberrations with radial actuators. The influence of normal actuators and their ability to correct for astigmatism based on modeling-directed actuator changes was first examined. Since the normal actuators are to only push on the contact ring, all the actuators were stroked in approximately 20 microns to establish a bias. This provided a reasonable amount of positive and negative stroke as dictated by the modeling results. This new shape after removing the focus and spherical terms was then passed over to IODA which uses the Finite Element Method (FEM) generated influence functions to calculate the required actuator strokes to obtain the minimized error shape. Several iterations had

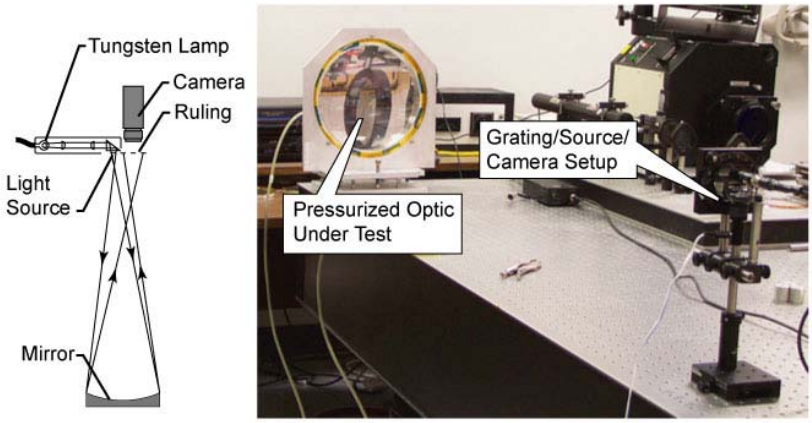

Figure 3. Schematic and Actual Setup of Ronchi Test

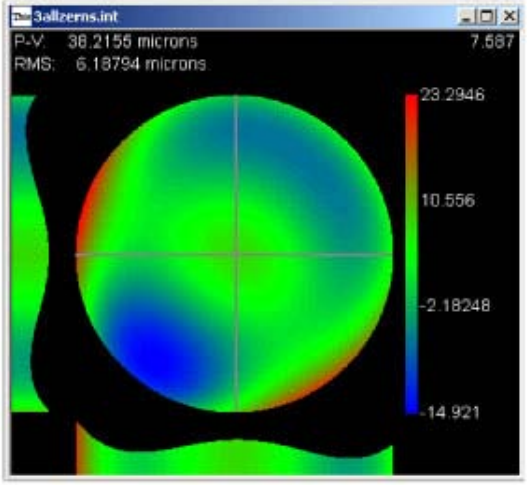

1st Order Zernike Term	Aberration (Microns)
Astigmatism-X	4.00
Astigmatism-Y	10.09
Coma-X	-0.57
Coma-Y	0.35
Spherical	7.28

Figure 4. Membrane shape with Focus Term Removed and Realistic Aberration Magnitudes

Actuator	Iteration (Actuator Stroke in Microns)				
	1	*2*	*3*	*4*	*5*
1	-5.44	-1.38	2.64	0.22	0.12
2	-11.30	-2.88	-0.69	7.87	0.16
3	-9.12	-1.69	-3.25	5.21	0.10
4	1.20	6.05	1.17	-5.92	-0.03
5	8.30	10.02	5.70	-9.05	-0.06
6	7.49	2.88	1.51	-1.46	-1.11
7	4.91	-5.44	-4.51	5.05	-2.63
8	2.67	-6.23	-3.83	5.90	-0.94
9	-2.01	-4.63	-1.79	3.70	3.87
10	-6.34	-3.58	-2.06	-1.57	5.14
11	-6.34	1.29	1.84	-6.31	0.02
12	-4.43	6.85	7.95	-3.64	-4.68
13	-2.28	5.50	5.15	2.58	-3.28
14	2.62	0.60	-4.17	3.11	0.52
15	7.95	-0.86	-6.92	0.13	1.57
16	7.98	-1.12	-2.37	-0.34	0.69
17	4.07	-2.78	1.17	-1.51	0.32
18	0.14	-2.53	2.51	-3.92	0.27
X-Astigmatism Error (in microns)	-1.10	1.46	2.44	1.32	0.26
Y-Astigmatism Error (in microns)	-4.58	-1.63	0.92	0.70	0.20

Table 1. Successive Actuator Strokes in Microns for Each Iteration as Directed by IODA X and Y Astigmatism Error are Successively Reduced.

to be made to get to an approximation of the model directed actuation since simple thumbscrews were used as actuators, which could only provide an estimated amount of stroke. **Table 1** shows the successive actuator stroke iterations directed by IODA along with the resulting astigmatism error. By the fourth iteration the astigmatism has been significantly reduced and the actuations dictated by the model were too small to implement with the thumbscrews. **Figure 5** shows the initial shape error and the final shape error of the pressurized membrane after the iterations listed in **Table 1**; with only the astigmatism errors present to easily note the effect. The RMS surface error was reduced from 3.234 microns to 0.628 microns. The correlation between the influence functions and the resulting reduction in shape error make it clear that the model accurately predicts the actuation necessary to obtain a minimized error shape based only on the normal actuators.

Similar testing was also conducted using radial actuators to validate modeling predictions. **Figure 6** shows the membrane shape with the focus and rigid body terms removed from the last normal actuator adjustment and the shape of the membrane with additional adjustments made using the radial actuations directed by IODA. The amount of figure error decreased from 2.417 microns to 0.909 microns, with the main reduction coming from the coma term. More accurate actuation devices will be used in the 0.75-meter PAMM, which will further reduce the shape error by more closely matching the required actuation.

The test data on this 0.25-meter PAMM conclude that active boundary control has good control authority over astigmatism and coma aberrations as predicted by the modeling design studies. Studies showed that a PAMM will achieve slightly better imaging performance with an electrostatic pressure boundary control than a radial control. Therefore, the 0.75m mirror mount will utilize electrostatic pressure control (capable of 32 electrostatic force actuators located circumferentially around the outer 1 inch of the membrane outer diameter) coupled with boundary warping (32 out-of-plane normal actuators) to demonstrate the feasibility of boundary control. High voltage power supplies controlled by a LabView control panel will be used to demonstrate the electrostatic pressure control. To test out the electrostatic system prior to implementation on the 0.75-meter PAMM, the equipment was first tested on the existing 0.25-meter small-scale mirror mount using a full aperture control.

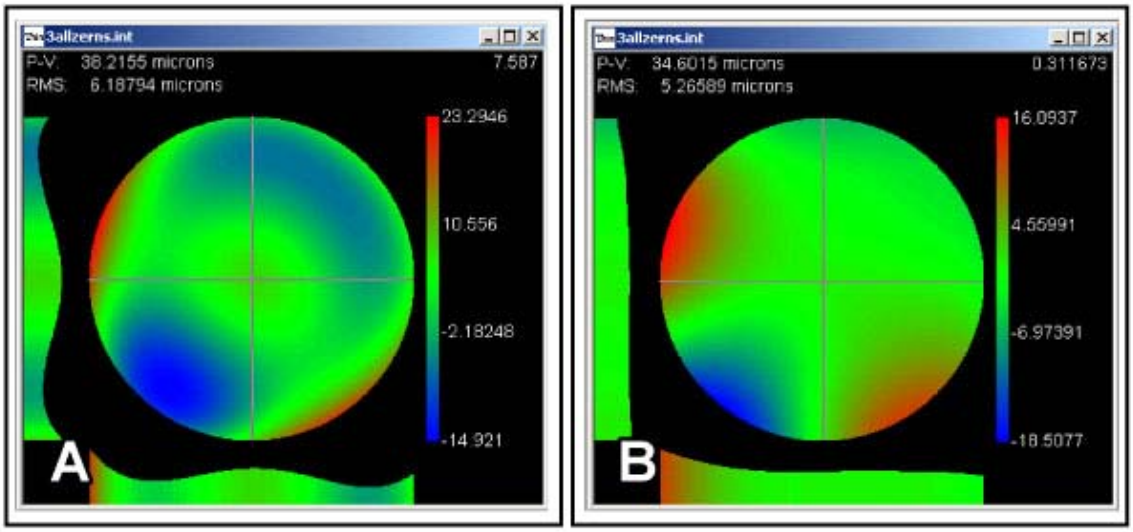

Figure 5. A) Initial Membrane Shape Error and B) Final Membrane Shape Error After Normal Actuator Iterations. Both Plots have First Order Focus, Spherical and Coma Removed to Clearly Show the Astigmatism Correction

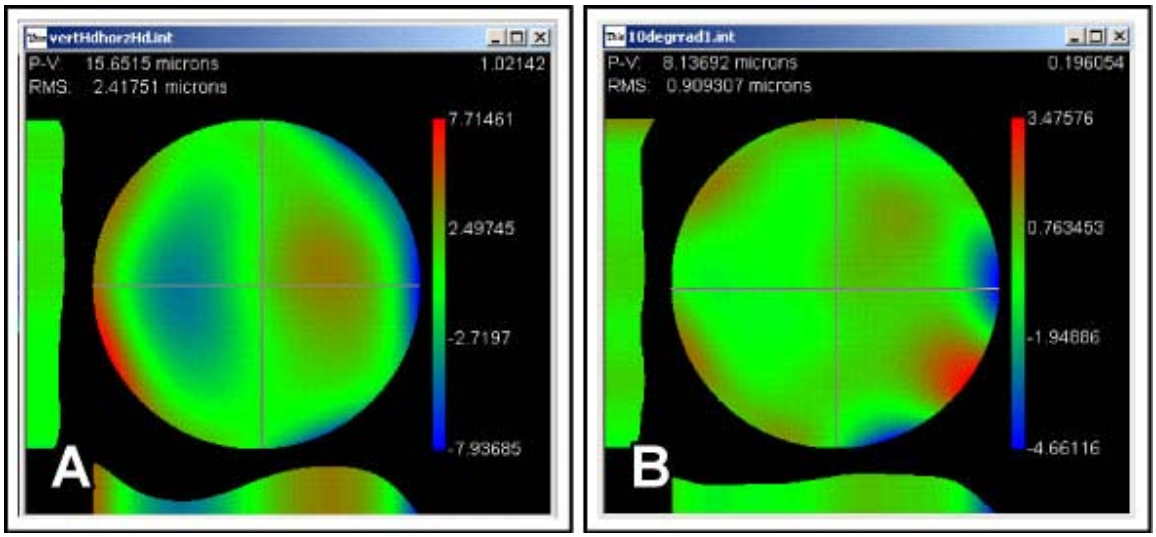

Figure 6. Membrane Shape Error A) After Normal Actuator Iterations and B) After Radial Actuator Iterations. Both Plots have Focus and First Order Spherical Terms

3. ELECTROSTATIC SETUP DEVELOPMENT

An electrostatic control along with normal actuators will be used to control the boundary of the 0.75m test article. In order to verify the suitability of high voltage power supplies for use in large electrode applications, and to characterize the membrane reaction to a large electrode, a test of large electrode and membrane was performed by applying it to a full aperture control on the 0.25m PAMM.

In this test setup, a 0.22m diameter electrode system was placed behind a 0.25m diameter membrane with radial and boundary warping control. The basic principle is to use electrostatic pressure to maintain the desired shape and correct

aberrations in the stretched membrane. A fourteen-electrode electrostatic control system was designed to demonstrate electrostatic control on the small-scale mount. This system is based around a National Instruments LabView control panel/ data acquisition card controlling a bank of 12 kV high voltage power supplies. The low level electrostatic functional block diagram combined with 0.25m PAMM is shown in **Figure 7.** The control computer allows the user to control the output voltage for each individual electrode from 0-12000 Volts on the 0.25-meter electrostatic backplane. The panel provides a proportional master slider to control voltages on all electrodes and also for each ring. The computer then scales down these voltages and outputs a 0-10 volts signal to the National Instruments PCI-6723 card. The card reads the analog signal, identifies the selected channel(s) and outputs the specified voltage to the corresponding high voltage power supply. To improve control of the high voltage power supplies, the wiring connectors for the power supplies incorporated feedback channels using a National Instruments PCI-6034E card to monitor the output voltage from the high voltage power supplies.

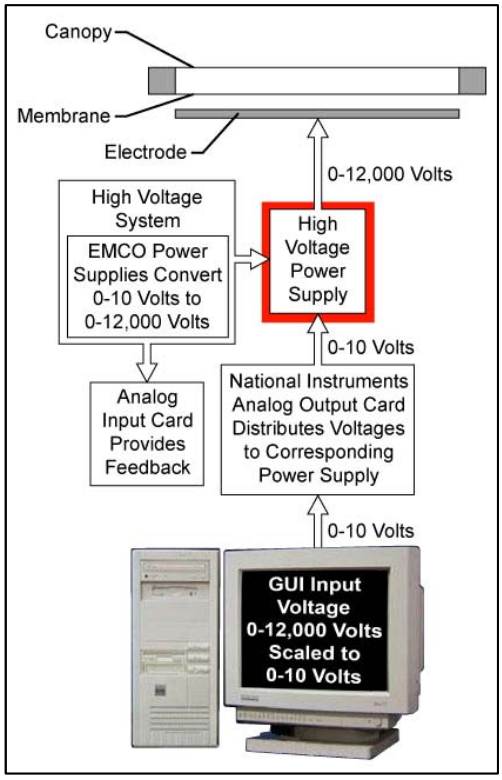

Figure 7. PAMM Hardware and Electrostatic Control Block Diagram

Modeling studies conducted using FEM and IODA predicted that sufficiently high voltage (up to 12000 volts) is required to deform the mirror to the desired radius of curvature based on a selected gap of 4mm between electrode and membrane to prevent arcing. The electrode pad, shown in **Figure 8** has 14 electrodes in a keystone pattern to ensure full coverage of the membrane. The function of an electrode is to provide a conductive surface where the voltage can be individually controlled independent of other electrodes. Each electrode was a 50-micron (2mil) thick aluminum coated Kapton membrane adhesively attached to a plexiglass support disk. Insulating gaps to eliminate arcing between electrodes were created by stripping 2.54 mm (0.1") wide aluminum all around the edge of each electrode. This area was found to be small enough to have any effect on the figuring capability of the film.

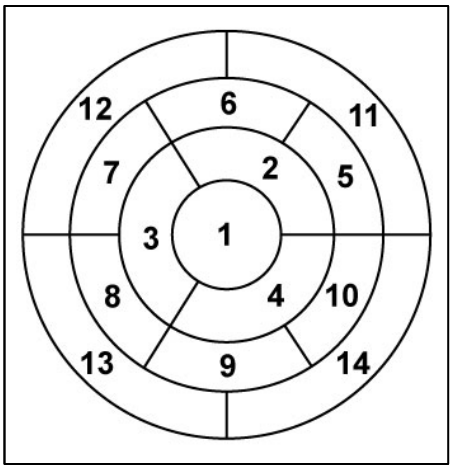

Figure 8. 14-Channel Electrode Pattern

A quick test was performed to determine the effect of arcing on the Kapton side of the film versus aluminum side of the film. In terms of the electrostatic attraction forces, there was very little difference in pressure between aluminum side facing and aluminum side away from membrane. However, it was found that having the Kapton film layer separate the membrane and the charged side of the electrode helped eliminate arcing. The arcing did not cause any damage to the Kapton side but when applied to the aluminum side patches of aluminum were removed both on the membrane and electrode wherever the arcing occurred. Following this experiment, it was concluded that the electrode would have the Kapton side facing the reflector film and the aluminum side facing away. Therefore, any arcing that might occur will not damage the electrode. A thick insulated high gage wire from high voltage power supply was attached to the electrode using conductive adhesive. Similarly, the membrane support ring was connected to the ground terminal using a small gage wire. **Figure 9** shows the integrated control hardware and the 0.25m diameter PAMM to form the electrostatic test setup.

The membrane was pressurized to obtain the design 1.63m radius of curvature and a Ronchi test was setup to obtain data. **Figure 10** shows the Ronchigrams and resulting optical path difference (OPD) plot for the membrane with no electrostatic pressure. With the focus term removed this plot shows the characteristic spherical error for an inflated membrane. The electrostatic system was then powered on and the voltages were manually adjusted to achieve the best shape by noting the changes in the Ronchigram. **Figure 11** shows the results. The lines in the Ronchigrams are notably

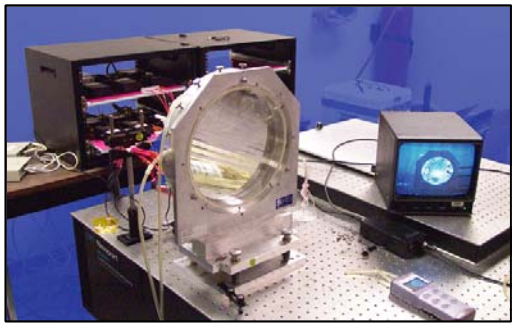

Figure 9. 0.25-meter PAMM Integrated with Electrostatic Control

straighter out to the edge, a result of reduced spherical aberration. There is some distortion though near the center of the Ronchigram that is due to some irregular peaks in the electrode film. These are located on the tabs that run through the acrylic to make the electrical connection. This can be corrected simply by creasing the electrode tab to make a clean contact between it and the acrylic surface. Nevertheless the resulting OPD shows the improvement in the membrane shape. The spherical aberration has been reduced from 5.9 to -0.6 microns.

The above testing ensured the proper functioning of high voltage power supply setup, the LabView GUI control panel and the large electrodes that can now be safely used in the boundary control of 0.75-meter diameter PAMM. In addition to boundary control, the 0.75m membrane will be coated with a variable thickness coating on the non-mirror side that should potentially improve the shape error of the membrane by deforming it to the desired curvature. Results of testing performed on a 0.25m diameter membrane mirror show that the variable thickness coating has improved the figure error.

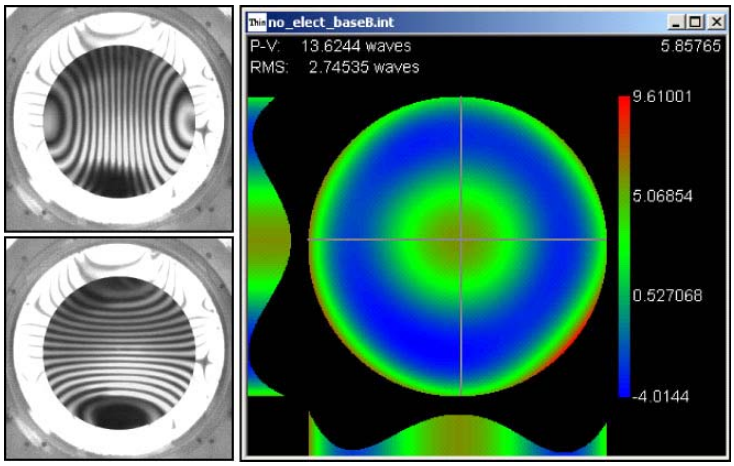

Figure 10. Membrane Shape Data with No Electrostatic Pressure

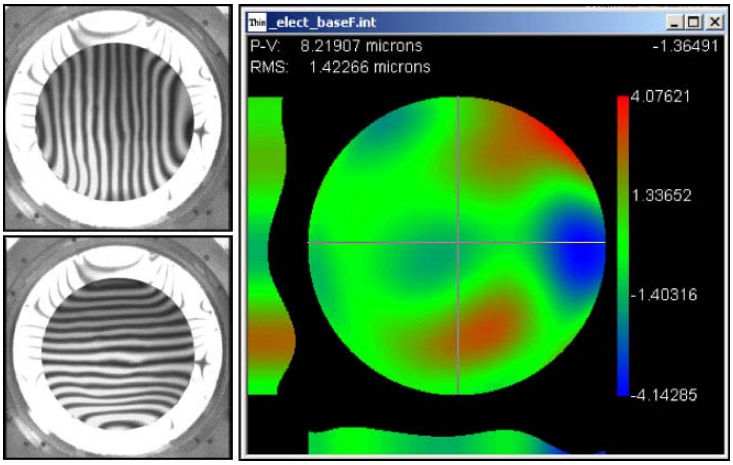

Figure 11. Membrane Shape Data with Electrostatic Pressure

4. VARIABLE THICKNESS COATED MEMBRANE MIRROR

The three dimensional theory of elasticity along with the method of asymptotic expansions are used to derive the mechanics of a coated membrane laminate[2]. The system of equations generalizing the Hencky-Campbell theory for a circular coated membrane laminate with clamped boundary conditions was already presented[3]. The coated membrane is assumed to be initially flat and a coating thickness distribution was derived that takes into account the axial and radial displacement of points deformed upon inflation. A power series solution to a nonlinear differential equation gives the coating thickness distribution required to deform a thin circular membrane subjected to transverse pressure, to a true paraboloidal surface as[4]

$$h_C(R) = h_0 + h_2(kR)^2 + h_4(kR)^4 + h_6(kR)^6 \qquad (1)$$

where the coefficients h_0, h_2, h_4 and h_6 are coefficients in the power series[3], k is the curvature of the desired parabola and R is the radial coordinate. This theory was applied to the 0.25-meter diameter mirror model containing a sandwiched multilayer-coated CP1 membrane with the properties specified in **Table 2.** The variable-thickness outer layer number 5 is another aluminum coating, which we assume has zero thickness at the center. The membrane is assumed to have an intrinsic tensile stress produced during the curing process, due to the CTE mismatch between it and a float glass mandrel upon which it is cast. The process used to coat CP1 membranes yields negligibly small intrinsic stress in the coatings. In **Figure 12** the coating thickness distribution for a true parabolic surface is plotted when the membrane shrinkage stress has the value 4899.97 psi and zero intrinsic stress in all the coatings.

Two coated membranes were included in the test. One film was coated using a standard uniformly thick reflective aluminum. This membrane was used as the baseline for comparison to the varied coating thickness test results. The second film was a CP1-DE mirror coated with the radially varying thickness coating distribution (coated on non-imaging surface). This membrane has the same production properties as the uniformly coated membrane (Same casting conditions, polymer batch, and thickness). The imaging side was coated with a uniform aluminum coating to allow proper image reflection. The graph shown in **Figure 13** compares the theoretical

Layer	Material	Thickness (m)	Poisson's Ratio	Young's Modulus (psi)	Intrinsic Stress (psi)
5	Aluminum	Variable	0·33	$10x10^6$	0
4	Nichrome	$50x10^{-10}$	0·33	$31x10^6$	0
3	CP1	$8x10^{-6}$	0·34	$315x10^3$	4,899.97
2	Nicrhome	$50x10^{-10}$	0·33	$31x10^6$	0
1	Aluminum	$700x10^{-10}$	0·33	$10x10^6$	0

Table 2. Geometrical and Material Properties of CP1 Sandwiched Between Aluminum and Nichrome Coatings. The Last Layer is a Variable-Thickness Aluminum Coating

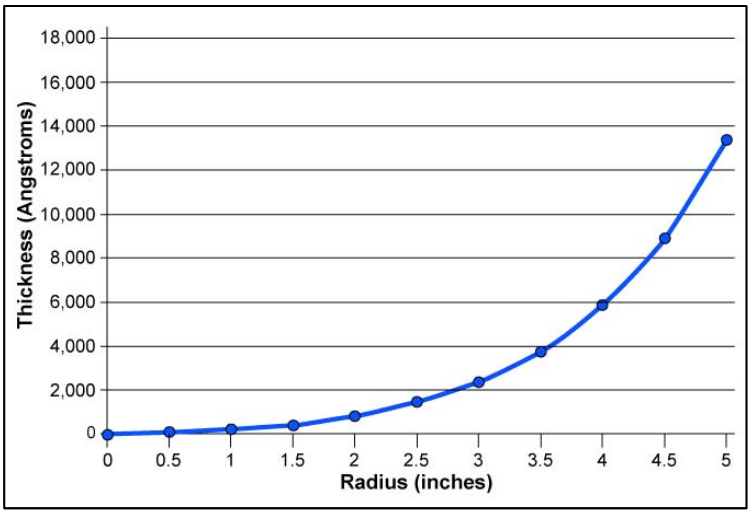

Figure 12. Plot of Theoretical Coating Thickness Profile

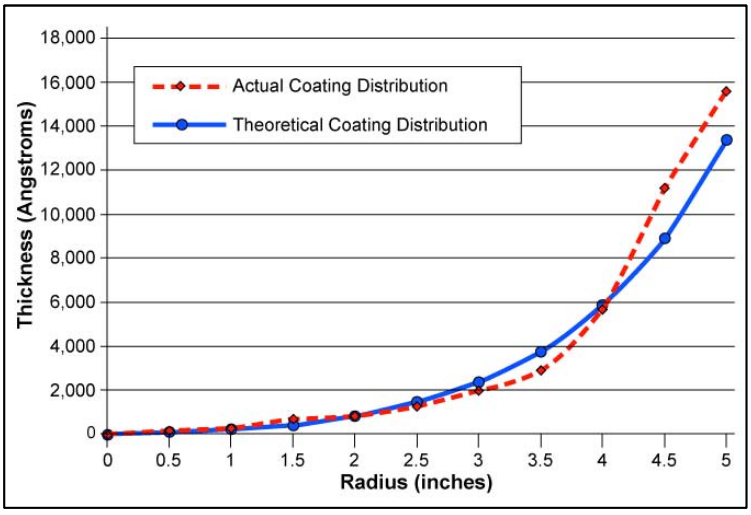

Figure 13. Plot of Theoretical and Actual Coating Thickness Profile

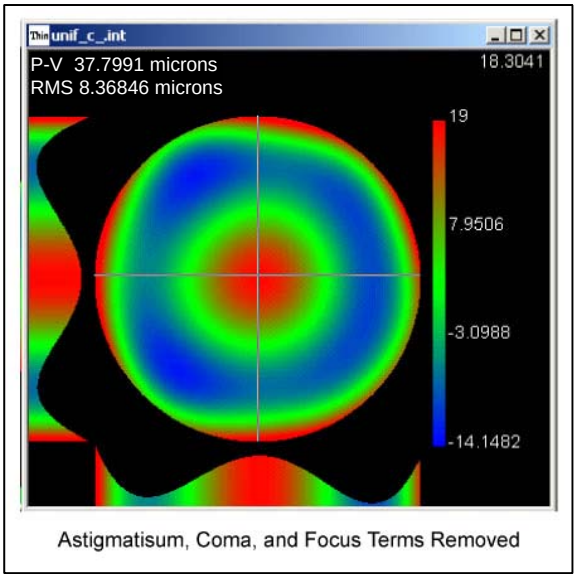

Figure 14. Membrane Shape for Uniformly Coated Mirror

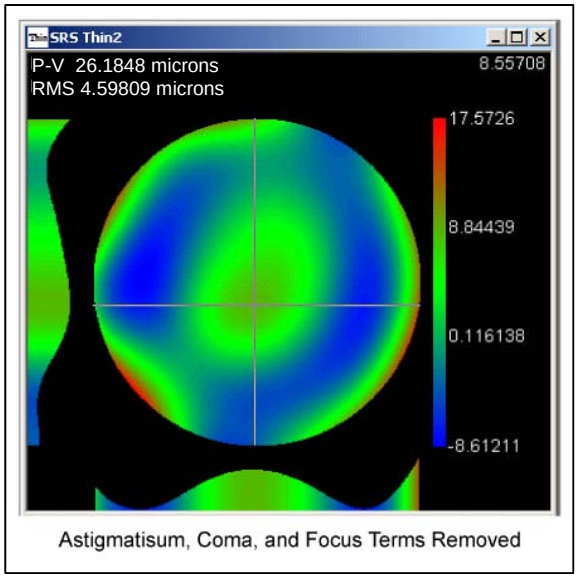

Figure 15 . Membrane Shape for Variable Thickness Coated Mirror

thickness profile and actual coated profile. Y-axis represents the normalized coating thickness; hence, 1 unit is equal to 1.6 microns coating thickness.

Figure 14 shows the analyzed data for the uniformly coated membrane mirror. These surface plots show the data compared to a flat. Astigmatism, coma, and the focus terms were removed to reveal the underlying spherical aberration. The classic "w" shape is revealed with a very clear trough along the circumference of the physical radius of the aperture. **Figure 15** shows the analyzed data for the varied stress coated membrane mirror after removing astigmatism, coma, and focus terms to verify the reduction in spherical aberration. These surface plots show the data compared to a flat. The varied stress coating resulted in a 54% decrease in spherical aberration after being pressurized to the design radius of curvature compared with the uniform stress coated mirror. It is anticipated that a more accurate coating match to the prescribed varied thickness coating will push the film back into an ideal parabolic shape. Due to the significant improvement in spherical aberration achieved in this test, this coating thickness distribution theory will be used for the 0.75-meter clear aperture PAMM.

5. SUMMARY AND CONCLUSIONS

It has been shown that boundary control using normal and radial actuation techniques can significantly reduce the overall aberration on a membrane mirror inflated from an initially flat state. The remaining spherical error can be reduced by using a varied thickness stress coating application on the membrane to change the mechanical properties of the material so that it forms more into a parabolic shape upon inflation. Any remaining spherical error can be corrected downstream. Successful model correlation has been conducted on a 0.25 meter test article for both boundary control as well as electrostatic figure control. The data summarized in this paper will now be used to help with initial testing of a 0.75 meter lenticular membrane mirror system to demonstrate minimal spherical aberration for use as a lightweight imaging optic.

6. REFERENCES

1. J. Moore , B. G. Patrick, S. Chodimella, D. Marker, A. Maji , "Development of a One-Meter Membrane Mirror with Active Boundary Control", SPIE Proceedings, vol. 5553: Advanced Wavefront Control: Methods, Devices, and Applications II, pp. 221-229, October 2004.

2. Murphy, L. M., “Moderate axisymmetric deformations of optical membrane surfaces,” *Journal of Solar Energy Engineering*, Vol. 109**,** May 1987, p. 111-120.
3. Hencky, H., “On the stress state in circular plates with vanishing bending stiffness”, *Zeitschrift für Mathematik und Physik*, Vol. 63, 1915, p. 311-317.
4. Campbell, J. D., “On the theory of initially tensioned circular membranes subjected to uniform pressure”, *Quart. J. Mech. & Applied Math.*, Vol. IX, Pt. 1, 1956, p. 84-93.